

Non-invasive analysis of actinic keratosis using a cold stimulation and near-infrared spectroscopy

Original

Non-invasive analysis of actinic keratosis using a cold stimulation and near-infrared spectroscopy / Seoni, S.; Veronese, F.; Tarantino, V.; Zavattaro, E.; Salvi, M.; Michielli, N.; De Santi, B.; Molinari, F.; Savoia, P.; Meiburger, K. M.. - ELETTRONICO. - 2019:(2019), pp. 467-470. (41st Annual International Conference of the IEEE Engineering in Medicine and Biology Society, EMBC 2019 Berlin, Germany 23-27 July 2019) [10.1109/EMBC.2019.8857279].

Availability:

This version is available at: 11583/2931565 since: 2021-10-18T10:50:24Z

Publisher:

Institute of Electrical and Electronics Engineers Inc.

Published

DOI:10.1109/EMBC.2019.8857279

Terms of use:

This article is made available under terms and conditions as specified in the corresponding bibliographic description in the repository

Publisher copyright

IEEE postprint/Author's Accepted Manuscript

©2019 IEEE. Personal use of this material is permitted. Permission from IEEE must be obtained for all other uses, in any current or future media, including reprinting/republishing this material for advertising or promotional purposes, creating new collecting works, for resale or lists, or reuse of any copyrighted component of this work in other works.

(Article begins on next page)

Non-invasive analysis of actinic keratosis using a cold stimulation and near-infrared spectroscopy

Silvia Seoni, Federica Veronese, Vanessa Tarantino, Elisa Zavattaro, Massimo Salvi, Nicola Michielli, Bruno De Santi, Filippo Molinari, *Member, IEEE*, Paola Savoia, Kristen M. Meiburger

Abstract— Non-melanoma skin cancers are the most common tumor in the Caucasian population, and include actinic keratosis (AK), which is considered an early form of *in-situ* squamous cell carcinoma (SCC). Currently the only way to monitor lesion progression (i.e., from AK to invasive SCC) is through an invasive bioptic procedure. Near-infrared spectroscopy (NIRS) is a non-invasive technique that studies haemoglobin (oxygenated haemoglobin, O₂Hb, and deoxygenated haemoglobin, HHb) relative concentration variations. The objective of this study is to evaluate if AKs present a different vascular response when compared to healthy skin using time and frequency parameters extracted from the NIRS signals. The NIRS signals were acquired on the AKs and a healthy skin area of patients (n=53), with the same acquisition protocol: baseline signals (1.5 min), application of ice pack near lesion (1.5 min), removal of ice pack and acquisition of vascular recovery (1.5 min). We calculated 18 features to evaluate if the vascular response was different in the two cases (i.e., healthy skin and AK lesions). By applying the multivariate analysis of variance (MANOVA), a statistically significant difference is found in the O₂Hb and HHb after the stimulus application. This shows how the NIRS technique can give important vascular information that could help the diagnosis of a lesion and the evaluation of its progression. Overall, the obtained results encourage us to look further into the study of the skin lesions and their progression with NIRS signals.

I. INTRODUCTION

Non-melanoma skin cancers (NMSCs) are the most common human cancer and they have the highest rate of tumour occurrence in the Caucasian population [1]. A common kind of skin lesion is actinic keratosis (AK), which usually represents an early form of *in-situ* squamous cell carcinoma (SCC) [2] [3]. In general, the tumor growth is influenced by sunlight exposure (and consequently by use of sunscreen) [4], genetic factors, age, gender and skin phototype. AK lesions appear in chronically sun-exposed

areas of the body such as the face, scalp, ears, forearms and hands, which is why the intensity but also the chronic nature of sunlight exposure plays a crucial role in the pathogenesis of the AK. The exposition to UVB is more dangerous than UVA and UVC: a long exposition to UVB could generate direct mutagenic effects on the DNA. Tumor growth is influenced also by immunosuppression therapies, which is why organ transplant patients (OTPs) show a higher risk of developing NMSCs [5]. An early treatment of AKs is fundamental to prevent or reduce the risk of progression of an AK lesion into SCC.

Currently the only technique to monitor the progression of these lesions (i.e., from AK to SCC) is an invasive bioptic procedure. It is widely accepted that angiogenesis is a phenomenon that is present in the onset and evolution of solid tumors. Since AK is an *in-situ* neoplasm, it can be expected that there could be a difference in the oxygenation state of the skin between AKs and healthy skin. In order to study this, NIR spectroscopy can be used, which is a non-invasive technique that studies relative concentration changes in oxygenated and deoxygenated hemoglobin (O₂Hb and HHb, respectively). The NIRS signal is highly non-stationary, non-Gaussian and nonlinear in nature, but it could give information about oxygenation of the lesioned skin. In fact, NIR spectroscopy has various medical applications [6] and has been used in the study of numerous pathologies, such as the evaluation of neurological diseases (such as Alzheimer's disease [7]) and cognitive aging [8], and the quantitative assessment of muscle metabolic pattern [9]. This method may be used to diagnose and prevent cancer [10], such as skin cancer [11], [12]. In these previous studies, the near-IR spectra were acquired on the lesion and control (healthy skin) and these showed the presence of significant spectral differences between them. The results were indicative of a different oxygenation and blood flow. In our current study, we added the cold stimulus application to improve the discrimination between healthy and lesioned skin.

The aims of this study are to evaluate the different oxygenation state between healthy skin and AKs lesions and to verify if a non-invasive NIRS technique can give information about the vascular response and be useful to monitor the progression of skin lesions.

The paper is organized in the following way: Section II presents a description of the methods used, section III shows the results that are then discussed in section IV.

S. Seoni, M. Salvi, N. Michielli, B. De Santi, F. Molinari and K.M. Meiburger, are with the PoliTo^{BIO}Med Lab, Department of Electronics and Telecommunications, Politecnico di Torino, Torino, Italy. (corresponding author to provide e-mail: silvia.seoni@polito.it).

F. Veronese, V. Tarantino and P. Savoia are with the Dermatology Unit, Dept. of Health Science, University of Eastern Piedmont, Novara, Italy.

E. Zavattaro is with the Dermatology Unit, Dept. of Translational Medicine, University of Eastern Piedmont, Novara, Italy.

II. MATERIALS AND METHODS

A. Data acquisition

A commercial device (NIRO® 200-NX, Hamamatsu) was used to acquire NIRS signals. The unit uses near-infrared to measure the changes in the relative concentration of oxygenated haemoglobin (O₂Hb), deoxygenated haemoglobin (HHb) and total haemoglobin (Δ cHb). The NIRS signals were acquired on 53 patients (76 ± 20 years, range 51-92 years). The protocol was approved by the local ethics committee and all patients signed an informed consent before being included in the study. The signals were acquired at a sampling rate of 5 Hz and the emission and detection probe were placed on the skin at 2.5 cm distance from each other. The radiations follow a ‘banana-shape’ path through the skin, so the probes were placed closely together to analyze only the superficial layers of the skin. To evaluate the different vascular response of tissue, we tested the following protocol on all patients: acquisition of baseline signals (1.5 min), application of ice pack near probes (1.5 min), removal of ice pack and acquisition of vascular recovery (1.5 min). The analyzed skin areas were two for each patient: healthy skin area and AK lesion before any treatment. In the case of an AK lesion, the probes were placed so the lesion was positioned right in between the two probes. For the healthy skin area, the probes were positioned on the underside of the arm (while relaxed). Fig. 1 shows an example of AK lesion (1A), the placement of the probes (1B) and the HHb and O₂Hb signal in the AK and healthy skin (1C, 1D).

The AK lesions were always diagnosed by an expert dermatologist with 10 years experience through a portable dermatoscope (HEINE DELTA®20 T, Heine Optotechnik,

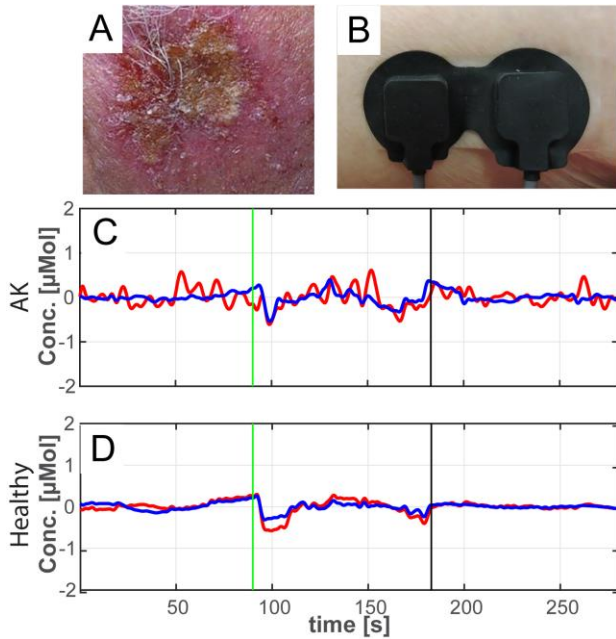


Figure 1. First row: example of AK (A), and placement of the probes (B). Second and last row: example of HHb and O₂Hb signals in AK lesion (C) and healthy skin (D). In (C, D) figures the signals HHb are blue and the O₂Hb signal are red.

Herrsching, Germany) visible analysis or an invasive bioptic procedure.

B. Pre-processing

All signals were filtered to remove any frequency components outside the range 10mHz-250mHz (5th order Chebyshev filter). The duration of the signals was 4.5 ± 0.5 min and the signals were divided in three epochs: *before* (before the application of the ice pack), *ice* (during the stimulus of the ice pack) and *after* (after removing the ice pack). We analyzed the concentration changes of HHb and O₂Hb signals in each epoch.

C. Feature extraction

The feature extraction was employed on both the O₂Hb and HHb signals. We extracted 18 features that were divided into two categories: time and frequency domain. Specifically, the features that we calculated were, in the time domain, the signal mean, variance, median, maximum, peak to peak amplitude, skewness, kurtosis, Hjorth mobility, Hjorth complexity, approximate entropy, average rectified value, RMS, energy, and number of zero crossings. For the computation of the approximate entropy (ApEn) we set $m = 2$ and r equal to 0.2 times the standard deviation of the signal as reported in [13]. The frequency domain features were the spectral entropy, the mean frequency, and the power in two bands of interest. The frequency bands of interest were the very low-frequency (VLF=20mHz-60mHz) and low-frequency (LF=60mHz-140mHz) bands. The power in the frequency bands was calculated using a time-frequency transform with a Choi-Williams exponential-type kernel ($\sigma = 0.5$). Moreover, the VLF and LF power bands were calculated on the whole signal (*before*, *ice* and *after* epochs) as well as within each epoch, considering both oxygenated and deoxygenated haemoglobin.

All features were calculated in each epoch of the analyzed signals (*before*, *ice* and *after*) and the mathematical description of each features adopted in this work is reported in Tab 1.

D. Statistical analysis

The HHb and O₂Hb signals were split into two groups: healthy skin and lesion. We calculated the 18 features on each signal for each group and then applied the multivariate analysis of variance (MANOVA) to evaluate if there was a statistically significant difference between the two groups. The MANOVA canonical variables are linear combinations of the original time and frequency features and are constructed so as to maximize the variance among groups. The p-value and MANOVA dimension (d) were used to determine if the two groups showed statistically significant differences ($p < 0.05$) and can be considered as belonging to two separate groups. We compared the same signal at the healthy skin area and at the AK lesion within each single epoch in depth: O₂Hb and HHb in *before*, *ice* and *after*.

Table 1. Mathematical description of features

Feature name	Mathematical description
Mean	$\bar{x} = \frac{1}{N} \sum_{i=1}^N x_i$
Variance	$var(x) = \frac{1}{N} \sum_{i=1}^N (x_i - \bar{x})^2$
Median	Middle value of ordered numbers
Maximum	The maximum value of time series
Peak-to-peak Amplitude	Difference between the maximum positive and negative amplitudes
Skewness	$skew(x) = \frac{\frac{1}{N} \sum_{i=1}^N (x_i - \bar{x})^3}{(\sqrt{var(x)})^3}$
Kurtosis	$Kurt(x) = \frac{\frac{1}{N} \sum_{i=1}^N (x_i - \bar{x})^4}{(var(x))^2}$
Hjorth Mobility	$HM(x) = \sqrt{\frac{var\left(\frac{dx}{dt}\right)}{var(x)}}$
Hjorth Complexity	$HC(x) = \frac{HM\left(\frac{dx}{dt}\right)}{HM(x)}$
Approximate Entropy	$ApEn = \frac{1}{N-(m-1)} \sum_{i=1}^{N-(m-1)} \ln C_i^m(r) - \frac{1}{(N-m)} \sum_{i=1}^{N-m} \ln C_i^{m+1}(r)$
Average Rectified Value (ARV)	$ARV(x) = \frac{1}{N} \sum_{i=1}^N x_i $
RMS	$RMS(x) = \sqrt{\frac{1}{N} \sum_{i=1}^N x_i ^2}$
Energy	$E(x) = \frac{1}{N} \sum_{i=1}^N x_i ^2$
Number of Zero Crossing	Number of times the signal crosses x-axis
Power VLF	P_{VLF} , The relative spectral power between 20mHz-60mHz
Power LF	P_{LF} , The relative spectral power between 60mHz-140mHz
Spectral Entropy	$SE = \sum_{i=1}^N p_i \cdot \ln \frac{1}{p_i}$
Mean Frequency	$MNF = \frac{\sum_{i=1}^N P_i \cdot f_i}{\sum_{i=1}^N P_i}$

P is power spectrum; f_i is the frequency; p is normalized power spectrum; $C_i^m(r)$ is the correlation integral; r is the criterion of similarity

III. RESULTS

In order to assess the presence of significant difference between healthy skin and AKs lesions, we applied the MANOVA in the three separate epochs to understand when the two signals show different behaviour, so as to analyze the influence of the stimulus application. Figure 2 displays the first two canonical variables as calculated by MANOVA for the three separate epochs.

The *before* epochs did not present significant differences ($d=0$, p -value >0.05), showing that in this case it is not possible to reject the null hypothesis that the two skin areas belong to the same group. Contrarily, in both the *ice* and *after* epochs the p -value was less than 0.05 both in HHb and O₂Hb signals and presented a $d=1$. This confirms that, in this case, we can reject the null hypothesis and therefore the skin areas can be divided into two separate groups and the first canonical variable is sufficient to discriminate between healthy and AK skin areas.

The highest three discrimination features of each epoch are listed in Tab. 2. The epoch with * had a p -value <0.05 , showing a statistically significant difference between the healthy skin area and the AK lesion area.

IV. DISCUSSION AND CONCLUSIONS

The proposed study has demonstrated that there is a vascular response difference between healthy skin and AK lesions following a cold stimulation. The stimulus (ice pack application) was an important point to see statistically significant differences. In fact, considering the epoch before the application of the ice pack, both the O₂Hb and HHb showed a similar behaviour, with a p -value greater than the significance level (0.05) and $d=0$. These results displayed that in basal conditions, the vascular response of the healthy skin and AKs lesions were similar. Instead, the results changed after the application of the stimulus, showing a $d=1$ and therefore that the two skin areas belong to two separate groups.

We can therefore conclude that the healthy skin and AKs lesions showed a different vascular response after the ice pack application, but not in basal conditions without any stimulation. This can be explained by the fact that a cold stimulation induces an initial vasoconstriction and a subsequent vasodilation, generating a difference between how the healthy skin vasculature responds when compared to the vasculature underlying an AK lesion. Considering the O₂Hb signal in the *after* epochs, the higher discrimination features were frequency features (VLF and LF bands). This shows that considering this signal, an important contribution is given by the rhythmic modifications of vessels diameters (P_{VLF}) and the vascular regulation of the autonomic nervous system (P_{LF})[14],[15]. Instead, in the HHb signals, the higher discriminant features were in the time domain: the Hjorth complexity, mean value and approximate entropy. The Hjorth complexity represents the contribution of the signal's change

Table 2. The three most discriminant features as calculated by MANOVA, * denotes a statistically significant difference.

Signals	Feat. 1	Feat. 2	Feat. 3
O ₂ Hb before	RMS	ARV	HC
HHb before	HM	HC	PLF
O ₂ Hb ice*	RMS	ARV	HC
HHb ice*	HC	P _{VLF}	PLF
O ₂ Hb after*	Median	P _{VLF}	PLF
HHb after*	HC	Mean	ApEn

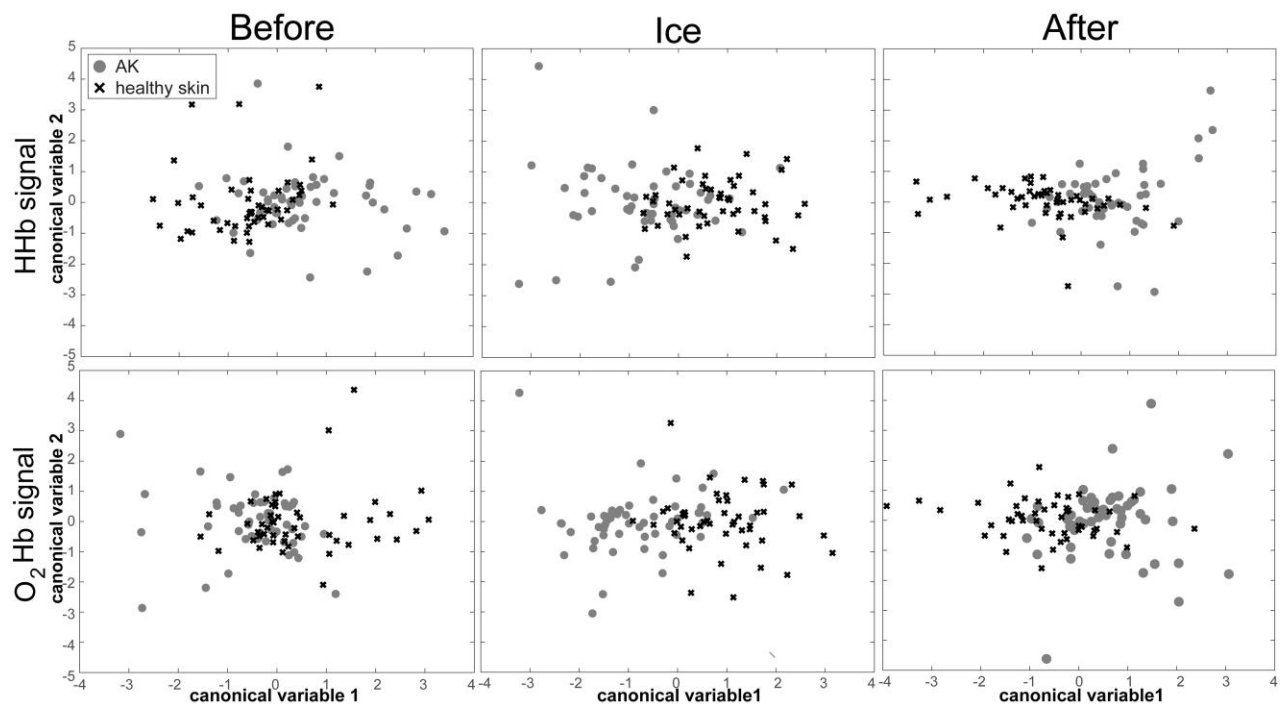


Figure 2. The first two canonical variables of the features on HHb and O₂Hb signals as calculated by MANOVA

in frequency, showing how it is not as much the single contribution in the different power bands that differentiates the two groups but rather how much the power band contributions change during the acquisition epoch.

This study showed that only NIR spectroscopy with the calculation of haemoglobin concentrations, without the application of the ice pack, did not give forth enough information. Instead, the use of NIR spectroscopy with the acquisition protocol has a clear potential in the non-invasive diagnosis of skin lesions. The acquisition protocol was easy for the health worker and it was not painful for the patients. The doctor, or a medical assistant, had to put two probes on the skin and acquire the signals. For the patient, the exam is comfortable and not painful. This protocol is a promising technique for the screening of the skin lesions. We are currently investigating the different vascular response after a specific treatment, in order to evaluate its effects. After this, the vascular response of the skin could return to its original condition, as healthy skin, or it could keep typical patterns of AKs lesions. Another interesting topic is the evaluation of progression of the AKs lesions. The AKs are the precursor of invasive SCC, and this protocol could help to classify the lesions (AKs or SCC) and to differentiate their grades. Overall, the obtained results encourage us to look further into the study of the skin lesions and their progression.

REFERENCES

- [1] S. J. Salasche, "Epidemiology of actinic keratoses and squamous cell carcinoma," *J. Am. Acad. Dermatol.*, vol. 42, no. 1 SUPPL. 1, pp. 4–7, Jan. 2000.
- [2] M. A. Mittelbronn, D. L. Mullins, F. A. Ramos-caro, and F. P. Flowers, "Frequency of pre-existing actinic keratosis in cutaneous squamous cell carcinoma," pp. 677–681, 1998.
- [3] J. Anwar, D. A. Wrone, A. Kimyai-asadi, and M. Alam, "The Development of Actinic Keratosis into Invasive Squamous Cell Carcinoma: Evidence and," 2004.
- [4] V. D. Criscione *et al.*, "Actinic keratoses," *Cancer*, vol. 115, no. 11, pp. 2523–2530, Jun. 2009.
- [5] M. Athar, S. B. Walsh, L. Kopelovich, and C. A. Elmetts, "Pathogenesis of nonmelanoma skin cancers in organ transplant recipients," *Arch. Biochem. Biophys.*, vol. 508, no. 2, pp. 159–163, 2011.
- [6] T. W. L. Scheeren, P. Schober, and L. A. Schwarte, "Monitoring tissue oxygenation by near infrared spectroscopy (NIRS): background and current applications," pp. 279–287, 2012.
- [7] P. Chou and T. Lan, "Journal of Clinical Gerontology & Geriatrics The role of near-infrared spectroscopy in Alzheimer's disease," vol. 4, pp. 12–15, 2013.
- [8] C. Wlodek, F. R. Ali, and J. T. Lear, "Use of Photodynamic Therapy for Treatment of Actinic Keratoses in Organ Transplant Recipients," vol. 2013, 2013.
- [9] F. Molinari, U. R. Acharya, R. Joy, R. De Luca, G. Petraroli, and W. Liboni, "Entropy analysis of muscular near-infrared spectroscopy (NIRS) signals during exercise programme of type 2 diabetic patients: Quantitative assessment of muscle metabolic pattern," *Comput. Methods Programs Biomed.*, vol. 112, no. 3, pp. 518–528, 2013.
- [10] V. R. Kondepoti and H. M. Heise, "Recent applications of near-infrared spectroscopy in cancer diagnosis and therapy," pp. 125–139, 2008.
- [11] R. K. Lauridsen, H. Everland, and L. F. Nielsen, "Exploratory multivariate spectroscopic study on human skin," pp. 137–146, 2003.
- [12] L. M. McIntosh *et al.*, "Towards Non-Invasive Screening of Skin Lesions by Near-Infrared Spectroscopy," no. January, 2001.
- [13] S. M. Pincus, "Approximate entropy as a measure of system complexity," *Mathematics*, vol. 88, no. March, pp. 2297–2301, 1991.
- [14] M. Salvi, D. Rimini, F. Molinari, G. Bestente, and A. Bruno, "Effect of low-level light therapy on diabetic foot ulcers: a near-infrared spectroscopy study," vol. 22, no. 3, 2019.
- [15] U. Sliwka, S. Harscher, R. R. Diehl, and R. Van Schayck, "Spontaneous Oscillations in Cerebral Blood Flow Velocity Give Evidence of Different Autonomic Dysfunctions in," no. Figure 1, 2001.